Proc. Natl. Acad. Sci. USA
Vol. 91, pp. 9146–9150, September 1994
Immunology

Human T-cell-mediated destruction of allogeneic dermal microvessels in a severe combined immunodeficient mouse

(heterologous graft/graft rejection/vascular endothelial cells/cytotoxic T lymphocyte/adhesion molecules)

ALLAN G. MURRAY*†‡, PETER PETZELBAUER*‡§¶, CHRISTOPHER C. W. HUGHES*†, JOSÉ COSTA†, PHILIP ASKENASE†‖, AND JORDAN S. POBER*†§**

*Molecular Cardiobiology Program, The Boyer Center for Molecular Medicine, and Departments of †Pathology, ‖Medicine, and §Immunobiology, Yale University School of Medicine, New Haven, CT 06510

Communicated by Vincent T. Marchesi, May 18, 1994

ABSTRACT **We developed a chimeric human-severe combined immunodeficient mouse model to study human allograft rejection. Mice received first partial thickness human skin grafts and then, after anastomosis of the mouse with graft human microvessels, human lymphocytes allogeneic to the skin. By 2 weeks, the skin grafts uniformly developed changes that resemble first-set skin rejection in humans. Vascular cell adhesion molecule 1 and major histocompatibility complex class II molecules were induced on the human vascular endothelium at day 6, prior to significant T-cell infiltration. Perivascular human CD4+ and CD8+ T-cell infiltrates were marked by day 11. Some T cells, adjacent to injured human vessels, expressed the cytolytic granule protein perforin. The human microvessels were destroyed by day 16 without significant damage to human keratinocytes or adjacent mouse microvessels. This small animal model may permit evaluation of potential therapeutic reagents that inhibit human T-cell-mediated injury.**

Microvascular endothelial cells (ECs) are thought to be the primary targets of acute allogeneic rejection reactions in vascularized allografts (1–3). Consequently, many therapeutic strategies are based on the concept of disrupting interactions between host T cells and graft ECs. However, many of the molecules that mediate such interactions are sufficiently different between humans and rodents that it has been necessary to use primates for the initial screening of inhibitory reagents. The human peripheral blood lymphocyte (PBL)–severe combined immunodeficient (SCID) mouse was introduced as a small animal model for studying the human immune system *in vivo* (4). C.B-17 mice homozygous for the SCID mutation are extremely inefficient at rearranging T- and B-cell antigen receptor genes (5, 6), and although natural killer (NK) cell function is intact, these T- and B-cell-deficient animals are unable to mediate rejection of human xenogeneic grafts. Upon introduction of human PBLs, such mice can respond to antigen by synthesizing human antibodies (4, 7–10). However, there has been little evidence that T-cell-mediated inflammatory reactions can develop in these animals (11–13), and human T cells may become anergic in the SCID mouse microenvironment (14).

We reasoned that a major part of the difficulty in reconstituting T-cell inflammatory function in the human PBL–SCID mouse may arise because murine ECs lack critical human cell surface proteins necessary for appropriate recruitment and activation of human lymphocytes. We grafted human skin with an intact dermal microvascular bed onto a SCID mouse prior to reconstituting the mouse with allogeneic human PBLs. Our model results in a reproducible stereotypic reaction in which human T cells infiltrate and destroy the human dermal microvessels, resembling first set skin graft rejection.

The publication costs of this article were defrayed in part by page charge payment. This article must therefore be hereby marked "*advertisement*" in accordance with 18 U.S.C. §1734 solely to indicate this fact.

MATERIALS AND METHODS

Animals. C.B-17 SCID mice (Harlan–Sprague-Dawley) were used at ages 5–8 weeks. The animals were housed in microisolator cages and were fed sterilized water and mouse chow. All experimental protocols were approved by the Yale Animal Care and Use Committee.

Antibodies. Rabbit anti-asialo G_{M1} for mouse NK-cell depletion was purchased from Wako Chemicals (Richmond, VA). The following antibodies were used for immunohistochemistry: mouse anti-human T cell (anti-CD3), mouse anti-human monocyte (anti-CD68), mouse anti-human Langerhans cell (anti-CD1a), mouse anti-human platelet–endothelial cell adhesion molecule (anti-CD31; Dako), hamster anti-mouse CD31 (gift from Steve Bogan, Boston University), mouse anti-human intercellular adhesion molecule 1 (anti-ICAM-1, RR 1/1; gift from T. Springer, Institute for Blood Research, Harvard University), mouse anti-human HLA-DR (LB3.1, gift from J. Strominger, Harvard University), mouse anti-human CD4 and mouse anti-human CD8 (Becton Dickinson), mouse anti-human vascular cell adhesion molecule 1 (anti-VCAM-1, E1/6; gift from M. P. Bevilacqua, Amgen Biologicals), and mouse anti-human E-selectin [H4/18 (15)], mouse anti-human perforin (T Cell Diagnostics, Cambridge, MA), and hamster anti-mouse CD3 (PharMingen). Biotin-conjugated *Ulex europaeus* agglutinin 1 (Dako) was also used for immunohistochemistry to identify human microvascular endothelium. The following antibodies were used for fluorescence cytometry: fluorescein isothiocyanate-conjugated mouse anti-human CD3 and mouse anti-human CD4, phycoerythrin-conjugated mouse anti-human CD8 (Exalpha, Cambridge, MA), and red 613-conjugated rat anti-mouse CD45 (GIBCO/BRL).

Peripheral Blood Mononuclear Cell (PBMC) Isolation and Engraftment. PBMCs were isolated from adult volunteer donors by leukopheresis (protocol approved by the Yale Human Investigations Committee) and purified using lymphocyte separation medium (Organon Teknika–Cappel). Approximately 3×10^8 cells were injected i.p. into each mouse. Where indicated, mice were pretreated by i.v. injection of 50 μl of anti-asialo G_{M1} antibody 12–24 h before PBMC engraftment.

Human Immunoglobulin and Circulating Lymphocyte Determination. Human IgG concentrations and circulating human lymphocyte frequency were determined from heparinized blood collected by retroorbital venipuncture. Human

Abbreviations: EC, endothelial cell; ICAM-1, intercellular adhesion molecule 1; PBL, peripheral blood lymphocyte; PBMC, peripheral blood mononuclear cell; SCID, severe combined immunodeficiency; VCAM-1, vascular cell adhesion molecule 1; NK, natural killer; H&E, hematoxylin/eosin; mAb, monoclonal antibody.

‡A.G.M. and P.P. contributed equally to this work.
¶Present address: Department of Dermatology, University of Vienna Medical School, A-1090 Vienna, Austria.
**To whom reprint requests should be addressed.

and mouse IgG levels were quantitated by a sandwich ELISA (16) using capture reagents and standards from Cappel (Durham, NC); the sensitivity of the assay was 100 ng/ml. Mice with detectable murine IgG levels were excluded from the studies. The frequency of circulating human T lymphocytes as a proportion of blood leukocytes was determined by fluorescence flow cytometry (FACSort; Becton Dickinson) (4). A live gate was established in the lymphocyte region and ≈10,000 events were recorded for analysis.

Skin Engraftment. Normal adult human breast skin was obtained as discarded tissue through the Yale University Department of Pathology (protocol approved by the Yale Human Investigations Committee). The superficial portions of the skin were harvested in 500- to 700-μm-thick sheets using a Goulian dermatome knife (gauge size, 0.016; Weck, Research Triangle Park, NC) and cut in approximately 7 × 7 mm pieces, which were kept in RPMI 1640 medium (GIBCO/BRL) at 4°C until transplantation. SCID mice were anesthetized by i.p. injection of Xylozine (3 mg/kg; Lloyd Laboratories, Shenandoah, IA) and ketamine (3 mg/kg; Aveco, Fort Dodge, IA). The skin was shaved, two 5 × 5 mm skin segments were excised from the back of each mouse, and the defects were immediately covered with the human skin grafts and fixed with disposable skin staples (3M, St. Paul). Grafts were individually harvested at the indicated times using the same anesthesia protocol.

Histology and Immunohistology. Each skin sample was used to prepare 3-μm paraffin-embedded sections stained with hematoxylin and eosin (H&E), and 4-μm cryostat sections were used for immunohistochemical staining (17). Controls used species-matched nonbinding monoclonal antibodies (mAbs) instead of specific mAbs.

Data Analysis. All skin specimens were evaluated by two observers. (*i*) The number of cells positive for human CD3, CD4, CD8, CD1a, and CD68 and mouse CD3 was assessed. A specimen was considered to show infiltration if the number of human leukocytes within the skin was at least 10-fold over that seen in the respective control specimen (i.e., human skin graft without reconstituted PBMCs in the same experiment). (*ii*) The expression of E-selectin, VCAM-1, ICAM-1, or HLA-DR was scored semiquantitatively (−, negative; +, discrete; ++, moderate; +++, strong). Tissue injury due to allogeneic PBMC reconstitution was assessed in paraffin-embedded specimens. Pooled data from three experiments are reported.

RESULTS

Engraftment of Human PBMCs to C.B-17 SCID Mice. Human PBMCs were engrafted into SCID mice as indicated by serum human IgG concentrations (≈1000 μg/ml at day 14) and by circulating human T cells. Human $CD3^+$ lymphocytes could be detected in the peripheral blood as early as 24 h after introduction into the peritoneal cavity. Preliminary experiments established the optimum number of PBMCs to be transferred as 3×10^8 cells (data not shown). Pretreatment of the mice with a polyclonal antibody to asialo-G_{M1} increased the frequency of circulating human T cells at days 3–14 (range, 1–60% of circulating leukocytes analyzed) without increasing human IgG concentrations when compared to saline-pretreated animals.

Histology of Human Skin Grafted on C.B-17 SCID Mice. Adult human skin grafts were routinely accepted by SCID mice (Figs. 1*A* and 2*A*). A critical consideration was that the dermis be as thin as possible yet retain the human dermal superficial vascular plexus. Seven days after engraftment, granulation tissue was evident at the base of the graft. Mouse and human capillaries (defined by double staining with anti-human CD31 and anti-mouse CD31 mAbs) appeared to

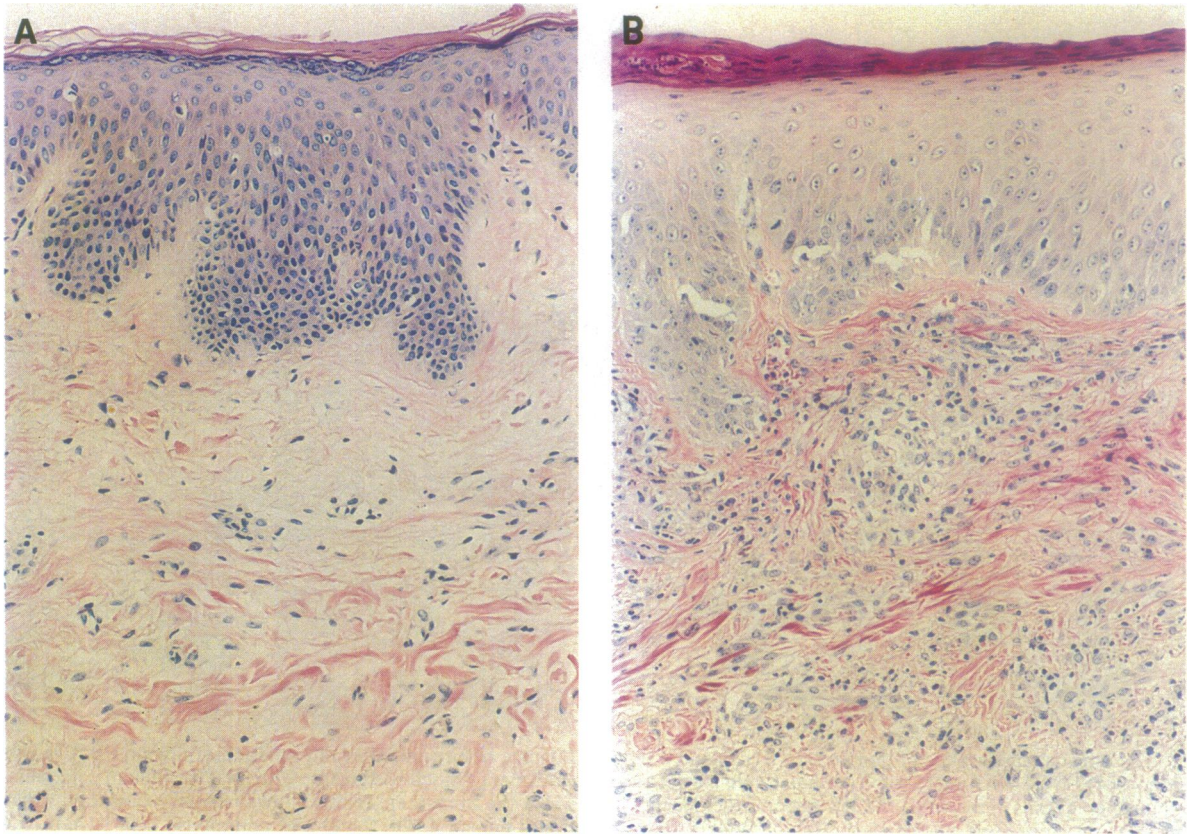

FIG. 1. Histological appearance of split-thickness human skin grafts harvested from SCID mice after reconstitution with allogeneic human PBMCs. (*A*) Micrograph of a day-16 control specimen harvested from an animal that received saline i.p. (*B*) Micrograph of a day-16 specimen harvested from a mouse that received allogeneic human PBMCs i.p. Each specimen was stained with H&E. Note the marked mononuclear infiltrate and focal loss of the dermal–epidermal junction in *B*. The mononuclear cells tend to be arranged in an angiocentric pattern. (×150.)

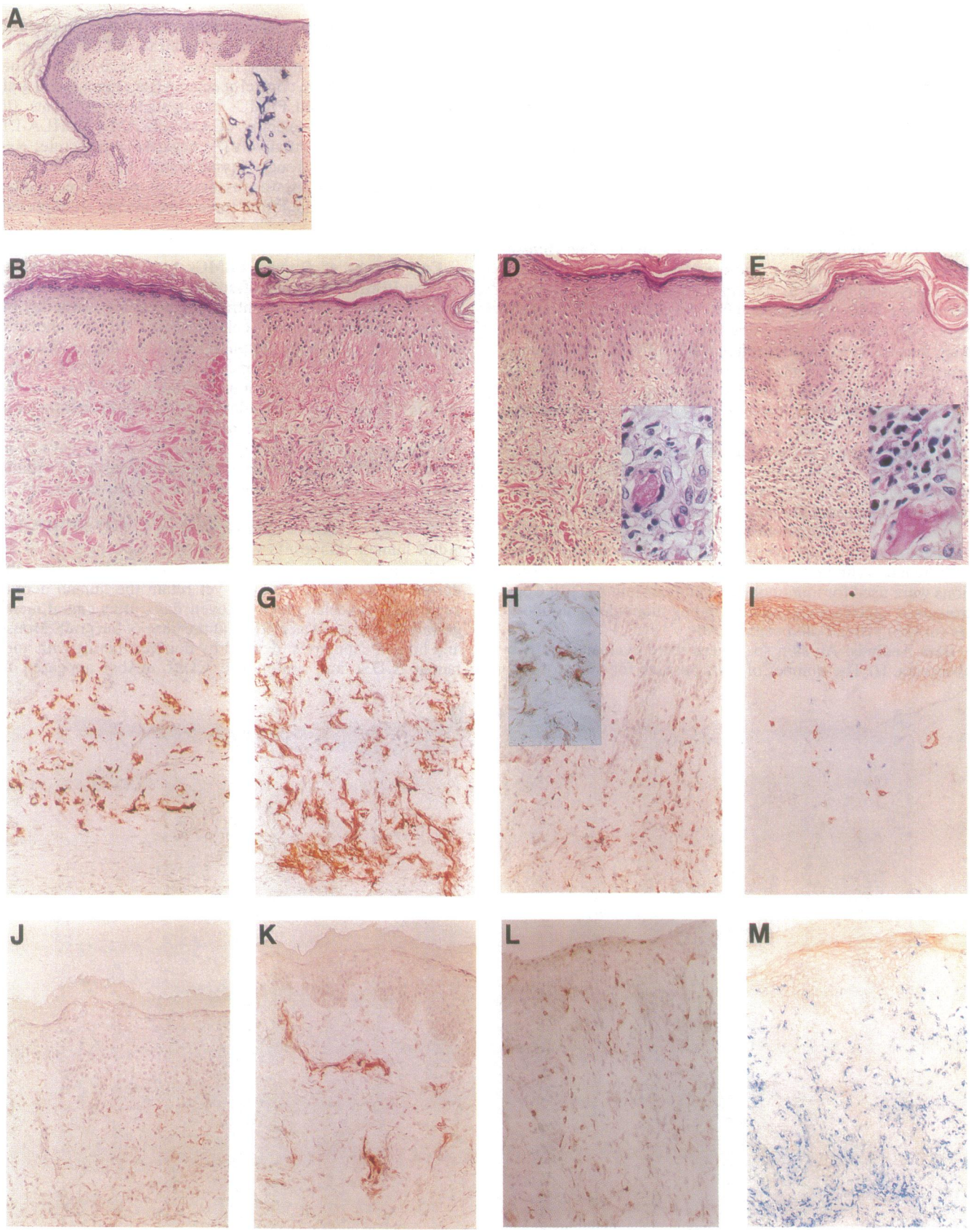

FIG. 2. Histological appearance of human skin transplanted onto SCID mice before and after introduction of human PBMCs allogeneic to the skin donor. (*A*) Low-power micrograph of human skin 2 weeks after engraftment stained with H&E. Note that the human epidermis is thicker than the mouse epidermis (present at the left edge of the specimen) and that the human epidermis shows normal maturation. There is little inflammation at the graft base at this time. (*Inset*) Double stained with anti-human CD31 (blue) and anti-mouse CD31 (red) to document microvascular anastomosis at the graft base. (*B–E*) H&E-stained micrographs of human skin harvested from SCID mice at 1, 6, 11, and 16 days, respectively, after introduction of human PBMCs allogeneic to the skin donor. Note the progressive infiltration of the dermis by mononuclear inflammatory cells beginning at day 6 (*C*) that fills the dermis by day 16 (*E*), while the epidermis is essentially uninvolved. (*D Inset*) Fibrin thrombus and perivascular proliferation of endothelial cells at high power in a day-11 specimen. (*E Inset*) Destruction of a human microvessel

intermingle, with focal evidence of microvessel anastomosis at the graft margins (Fig. 2*A Inset*). Human CD31$^+$ vessels persisted within the human dermis and contained intraluminal erythrocytes, indicating perfusion with mouse blood. The engrafted dermis retained small numbers of CD4$^+$ T cells and CD68$^+$ macrophages, and the epidermis retained CD1a$^+$ Langerhans cells. Few if any CD8$^+$ T cells were present.

Fourteen days after engraftment, the granulation tissue at the base of the human graft was largely resolved. Graft human CD31$^+$ microvessels persisted and occasional mouse CD31$^+$ vessels could be identified. The boundary between the human and mouse epidermis was sharply demarcated, and the human basal cell layer showed normal differentiation, except for focal areas with intercellular edema and rare single necrotic keratinocytes. The epidermal thickness was comparable to the pregraft specimen, and the rete peg pattern was well preserved. There was little evidence for immunological activation in the resting tissue. Human endothelium did not express E-selectin or VCAM-1 molecules. ICAM-1 and HLA-DR molecules were weakly expressed on the endothelium at levels comparable to pregraft specimens. Keratinocytes were HLA-DR-negative and ICAM-1 expression was detectable at very low levels on the basal keratinocytes.

Allogeneic Lymphocyte Response to Skin Grafts. A three-step protocol was developed to examine interactions between circulating human T cells and graft microvessels lined by human vascular endothelial cells. (*i*) Human skin was grafted onto SCID mice and allowed to heal for 14 days. (*ii*) Mice were treated with anti-asialo G_{M1} to deplete mouse NK cells. (*iii*) Twenty-four hours later, human PBMCs, allogeneic to the skin, were introduced i.p. This protocol produced a perivascular lymphocytic infiltrate in the skin grafts of >95% of the animals when studied at 16 days after the injection of human PBMCs (Fig. 1*B*). Introduction of PBMCs before or at the same time as skin engraftment led to an inflammatory infiltrate at the base of the graft that prevented mouse–human microvessel anastomosis.

Three time course experiments were performed with similar results. Skin grafts examined 1 day after PBMC reconstitution were indistinguishable from control specimens (Fig. 2*B*). By 6 days after PBMC reconstitution, three of five specimens showed focally damaged vessels characterized by dilated lumens, fibrin thrombi, and extravasated erythrocytes (Fig. 2*C*). Clusters of intraluminal human CD4$^+$ cells were adherent to the endothelium and some (score, +) CD4$^+$ and CD8$^+$ T cells were found in a perivascular distribution (Fig. 2*C*). The numbers of human CD68$^+$ macrophages and CD1a$^+$ Langerhans cells were indistinguishable from controls. Strikingly, in five of five specimens, HLA-DR (score, +++; Fig. 2 *F* and *G*) and VCAM-1 (score, ++; Fig. 2 *J* and *K*) were strongly up-regulated on most of the human dermal vessels. Endothelial ICAM-1 expression remained unchanged and E-selectin expression was not induced. Most human keratinocytes strongly (score, +++; Fig. 2 *F* and *G*) expressed HLA-DR, but keratinocyte ICAM-1 expression was not up-regulated on these cells.

By 11 days after PBMC reconstitution, the epidermis showed areas of marked acanthosis, although individual keratinocyte morphology was indistinguishable from day 1 (Fig. 2*D*). Five of five specimens showed infiltrates of human leukocytes. In three of five specimens, the infiltrate was moderate (score, ++) and in two of five, it was discrete (score, +). Infiltrates consisted of approximately equal numbers of CD8$^+$ cells (Fig. 2*H*) and CD4$^+$ (Fig. 2*L*) T cells, most of which expressed CD25 (data not shown). Macrophages and Langerhans cells appeared unaltered. Human blood vessels within the infiltrate were dilated; fibrin thrombi and extravasated erythrocytes were noted. Perforin-positive T cells were found in apposition to damaged ECs (Fig. 2*H Inset*). Adjacent areas contained knots of disorganized ECs, suggestive of proliferation (Fig. 2*D Inset*). VCAM-1 (score, +++) and HLA-DR (score, +++) on ECs were more strongly expressed compared to vessels observed on day 6. Furthermore, ICAM-1 (score, ++) was now strongly up-regulated on vascular ECs, but E-selectin was not detected. Keratinocyte HLA-DR was equal or diminished compared to the 6-day specimens (score, ++ to +++), whereas ICAM-1 was now up-regulated (score, ++).

By day 16 after PBMC reconstitution, the epidermis remained acanthotic and there was a focal epidermotropic T-cell infiltrate and disorganization of the basal cell layer with rare keratinocyte necrosis (Fig. 2*E*). Fifteen of 16 specimens showed strong (score, +++) human CD3$^+$ T-cell infiltrates, composed of equal numbers of CD4$^+$ and CD8$^+$ cells. Mouse CD3$^+$ T cells were not seen. Intact human blood vessels could no longer be identified (Fig. 2 *I* and *M*). In the residual human microvessels, the vessel wall was disrupted, with increased fibrin thrombi and extravasation of erythrocytes. Perforin-positive lymphocytes were again noted adjacent to the residual ECs. Many infiltrating T cells appeared as blasts, and multiple mitotic figures were evident. There was an increase in perivascular CD68$^+$ macrophages, but CD1a$^+$ Langerhans cells remained unchanged. CD31$^+$ endothelial remnants staining for VCAM-1, ICAM-1, or HLA-DR could not be readily distinguished from staining of infiltrating leukocytes. Keratinocyte expression of HLA-DR and ICAM-1 varied widely among specimens (score, + to +++).

DISCUSSION

This report describes a small animal model that may prove useful for the *in vivo* analysis of the human cell-mediated immune response to human allografts. We have introduced technical improvements into SCID mouse transplantation that (*i*) lead to perfusion of skin graft microvessels lined by human ECs and (*ii*) produce sustained circulating levels of human T cells. Specifically, we find that the use of split thickness adult skin, rather than neonatal foreskin specimens, leads to greater retention of the human microvessels (18). In addition, pretreatment of the mice with anti-asialo G_{M1} in conjunction with a large PBMC inoculum leads to higher levels of circulating human lymphocytes. When we combine these techniques, some of the circulating human T cells specifically localize to allogeneic skin grafts in a perivascular distribution but not to xenogeneic mouse skin. The human graft dermal microvasculature becomes activated coincident with the onset of T-cell infiltration, as indicated by the expression of VCAM-1 and major histocompatibility complex class II molecules. A subset of the human CD3$^+$ T

and proliferation of perivascular inflammatory cells in a day-16 specimen. (*F* and *G*) Staining with anti-HLA-DR antibody of specimens harvested at days 1 and 6, respectively, after the introduction of human PBMCs. Note that HLA-DR staining of dermal microvessels, some perivascular cells, and epidermal Langerhans cells are present on day 1. The staining intensity is increased by day 6 and HLA-DR is additionally expressed on keratinocytes. (*J* and *K*) Staining with anti-human VCAM-1 antibody at days 1 and 6, respectively. Note that VCAM-1 is absent at day 1 and is expressed on human dermal microvessels by day 6. (*H* and *L*) Stained for human CD8 and CD4, respectively, on day 11 specimens. (*H Inset*) Stained for human perforin. Perforin-positive cells are localized adjacent to human microvessels. (*I* and *M*) Double-stained with *Ulex europaeus* agglutinin 1 (red) to detect human endothelium and anti-human CD3 (blue) to detect T cells. (*M*) Specimen harvested 16 days after introduction of PBMCs. (*I*) Paired specimen from a mouse that did not receive PBMCs. Note that the inflammatory infiltrate in *M* is largely composed of human T cells and that at this time point, human endothelial cells have largely disappeared compared to the control specimen (*I*). (*A*, ×45; *B–M*, ×90; insets, ×180.)

cells differentiate to display a cytolytic phenotype marked by expression of the granule protein perforin, and by ≈2 weeks after reconstitution with allogeneic human PBMCs, the human microvasculature of the skin graft is destroyed.

Kawamura *et al.* (11) have described "chronic" human skin rejection in a SCID mouse model. In this system, skin grafts developed sclerosis and lymphocyte infiltration 3–4 weeks after adoptive transfer of presensitized, but not naive, human lymphocytes. Our experience differs in several respects. (*i*) We demonstrate 95% of the skin grafts are infiltrated by unsensitized allogeneic human T cells within a week of PBMC reconstitution. (*ii*) We demonstrate destruction of human vascular elements within the skin consistent with the time course seen in first set skin rejection in humans (1). (*iii*) We provide evidence suggesting that the infiltrating T cells are activated in response to alloantigen. Differences in the experimental protocols likely account for these discrepancies. Most critically, we allowed the skin grafts to heal prior to the introduction of allogeneic human PBMCs. This promotes perfusion of the skin graft through anastomosed human microvessels. In addition we treated our mice with anti-asialo G_{M1} antibodies to promote engraftment of the human PBMCs (10, 12, 19) and we transferred large numbers (3×10^8 cells) of freshly harvested unsensitized PBMCs to each mouse. This protocol enhances the probability that human T cells introduced into the peritoneal cavity of the mouse will circulate and contact the human skin graft microvasculature.

The interpretation that the destruction of the human dermal microvasculature is mediated by allogeneic T cells is supported by the following observations. (*i*) We find evidence of destruction of the human dermal microvasculature only in mice reconstituted with allogeneic human lymphocytes. This observation indicates that the vascular damage is the result of neither effects of graft ischemia nor of a xenogeneic immune response mediated by mouse NK cells or other leukocytes. (*ii*) A human T-cell infiltrate precedes the loss of the human endothelium in a temporal profile consistent with the activation and differentiation of T cells in the allogeneic setting. Activation of the dermal T cells is inferred from the expression of the high-affinity interleukin 2 receptor, CD25, a marker of T-cell activation. Moreover, a subset of infiltrating T cells demonstrates perforin-positive cytolytic granules consistent with classic T-cell-mediated cytotoxicity directed against the allogeneic endothelium. Furthermore, the functional effects of cytokines produced by activated T cells are evident by the induction of major histocompatibility complex class II and VCAM-1 on the vascular endothelium and by the induction of ICAM-1 and class II molecules on the keratinocytes in the epidermis. Finally, T-cell blasts with numerous mitotic figures are seen in the skin harvested at day 16, presumably proliferating in response to alloantigen stimulation. In a preliminary experiment, T cells recovered from an infiltrated skin graft proliferated *in vitro* in response to dermal microvascular endothelial cells cultured from the skin graft donor but not from a third-party donor.

Interestingly, in this system we do not observe frank necrosis of the epidermis. In this model, unlike traditional allogeneic skin allograft models, the graft enjoys a dual blood supply, derived from both the anastomosis of the remnant human microvascular arcades with mouse microvessels and from the ingrowth of new mouse vessels. As the human immune response develops, selective destruction of the human vascular elements ensues, but the epidermis remains viable, presumably nourished by the remaining mouse capillaries. Necrotic keratinocytes are observed only rarely, and Langerhans cells are preserved.

Our findings are histologically similar to the cell-mediated immune response that was reported after transplantation of human skin to an allogeneic donor (1). In those experiments, T cells accumulated in the dermis of the allogeneic skin graft in a perivascular distribution. This was accompanied by endothelial cell activation as judged by morphologic criteria and followed by destruction of the microvasculature. In contrast to what is seen in the current model, foci of skin necrosis developed, coalesced over ≈24 h, and culminated in sloughing of the graft. Significantly, only focal keratinocyte necrosis was observed. The authors interpreted these results to suggest that the graft loss was primarily the effect of specific destruction of the graft microvasculature and secondarily a combination of ischemia and granulocyte infiltration.

Our model provides the opportunity to observe the role of EC adhesion molecules in the development of human allograft rejection. As the immune response to the graft evolves, VCAM-1 is up-regulated early (by day 6), whereas ICAM-1 expression is induced later in the response, and E-selectin was not induced. These observations suggest that VCAM-1 may serve to recruit T cells to sites of inflammation in the skin.

In conclusion, we have developed a model of human microvascular cell injury induced by allogeneic T lymphocytes in a SCID mouse. Histological examination suggests that the injury is T-cell mediated, consistent with acute cellular rejection. This model will be useful in studies of endothelial-dependent human T-cell recruitment and activation. It may offer the opportunity to test antiinflammatory reagents, such as mAbs or chimeric proteins that may be species restricted.

We thank the Department of Pathology and the Comprehensive Cancer Center, Yale New Haven Hospital, for providing skin specimens, and the Pheresis Service of the Yale Blood Bank for performing the leukopheresis of human volunteers. Financial support for this work was provided in part through a grant from American Cyanamid to the Molecular Cardiobiology Program at the Boyer Center for Molecular Medicine, from National Institute of Allergy and Infectious Diseases (Grant R37-AI-12211) to P.A., and from a pilot grant (to P.A. and J.S.P.) from the Yale Skin Diseases Research Center (Grant P30-AR414942). A.G.M. is the recipient of a fellowship award from the National Kidney Foundation of Canada. P.P. is the recipient of a fellowship award from the Max Kade Foundation of Austria.

1. Dvorak, H. F., Mihm, M. C., Dvorak, A. M., Barnes, B. A., Manseau, E. J. & Galli, S. J. (1979) *J. Exp. Med.* **150**, 322–337.
2. Leszczynski, D., Lasczynska, M., Halttunen & Häyry, P. (1987) *Kidney Int.* **31**, 1311–1316.
3. Matsumoto, Y., McCaughan, G. W., Painter, D. M. & Bishop, G. A. (1993) *Transplantation* **56**, 69–75.
4. Mosier, D. E., Gulizia, R. J., Baird, S. M. & Wilson, D. B. (1988) *Nature (London)* **335**, 256–259.
5. Dorschkind, K., Keller, G. M., Phillips, R. A., Miller, R. G., Bosma, G. C., O'Toole, M. & Bosma, M. J. (1984) *J. Immunol.* **132**, 1804–1808.
6. Fulop, G. M. & Phillips, R. A. (1990) *Nature (London)* **347**, 479–482.
7. Carlsson, R., Martensson, C., Kalliomaki, S., Ohlin, M. & Borrebaeck, C. A. (1992) *J. Immunol.* **148**, 1065–1071.
8. Leader, K. A., Macht, L. M., Steers, F., Kumpel, B. M. & Elson, C. J. (1992) *Immunology* **76**, 229–234.
9. Hesselton, R. M., Koup, R. A., Cromwell, M. A., Graham, B. S., Johns, M. & Sullivan, J. L. (1993) *J. Infect. Dis.* **168**, 630–640.
10. Shpitz, B., Chambers, C. A., Singhal, A. B., Hozumi, N., Fernandes, B. J., Roifman, C. M., Weiner, L. M., Roder, J. C. & Gallinger, S. (1994) *J. Immunol. Methods* **169**, 1–15.
11. Kawamura, T., Niguma, T., Fechner, J. J., Wolber, R., Beeskau, M. A., Hullett, D. A., Sollinger, H. W. & Burlingham, W. J. (1992) *Transplantation* **53**, 659–665.
12. Murphy, W. J., Conlon, K. C., Sayers, T. J., Wiltrout, R. H., Back, T. C., Ortaldo, J. R. & Longo, D. L. (1993) *J. Immunol.* **150**, 3634–3642.
13. Rendt, K. E., Barry, T. S., Jones, D. M., Richter, C. B., McCachren, S. S. & Haynes, B. F. (1993) *J. Immunol.* **151**, 7324–7336.
14. Tary-Lehmann, M. & Saxon, A. (1992) *J. Exp. Med.* **175**, 503–516.
15. Pober, J. S., Bevilacqua, M. P., Mendrick, D. L., Lapierre, L. A., Fiers, W. & Gimbrone, M. A. (1986) *J. Immunol.* **136**, 1680–1687.
16. Macy, E., Kemeny, M. & Saxon, A. (1988) *FASEB J.* **2**, 3003–3009.
17. Petzelbauer, P., Bender, J. R., Wilson, J. & Pober, J. S. (1993) *J. Immunol.* **151**, 5062–5071.
18. Yan, H.-C., Juhasz, I., Pilewski, J., Murphy, G., Herlyn, M. & Albelda, S. M. (1993) *J. Clin. Invest.* **91**, 986–996.
19. Murphy, W. J., Bennett, M., Anver, M. J., Baseler, M. & Longo, D. (1992) *Eur. J. Immunol.* **22**, 1421–1427.